Russian Geology and Geophysics © 2019, V.S. Sobolev IGM, Siberian Branch of the RAS
Vol. 60, No. 4, pp. 400–413, 2019 *DOI:10.15372/RGG2019029* *Geologiya i Geofizika*

Reconstruction of Magma Flow in Permo–Triassic Intrusions of the Angara–Taseeva Syneclise (Siberian Platform) Based on Magnetic Susceptibility Anisotropy Data

A.V. Latyshev [a,b,✉], P.S. Ul'yakhina [a,b], R.V. Veselovskii [a,b]

[a] *Lomonosov Moscow State University, Leninskie Gory 1, Moscow, 119991, Russia*
[b] *Schmidt Institute of Physics of the Earth, ul. Bol'shaya Gruzinskaya 10, Moscow, 123242, Russia*

Received 21 November 2017; received in revised form 14 February 2018; accepted 1 March 2018

Abstract—Based on detailed studies of the anisotropy of magnetic susceptibility (AMS), the directions of magmatic-melt propagation have been reconstructed in large dolerite sills of the Angara–Taseeva syneclise. Half the sites studied showed a magnetic fabric of "normal" type, i.e., the minimum K3 axis of the AMS ellipsoid is orthogonal to the contact, and the other two axes lie in the plane of the intrusive body. Interpreting the orientation of the maximum K1 axis as the direction of the melt flow at such sites, we compiled a scheme of the main magma flow directions. The obtained results are generally consistent with the hypothesis of magma-feeding zone in the central, most downwarped part of the Angara–Taseeva depression. The distribution of the maximum axes of the AMS ellipsoid is different in sills and points to the existence of local intrusion centers. Intrusions with an AMS ellipsoid of "reverse" type are predominant on the periphery of the depression. The sites with a "normal" magnetic fabric do not demonstrate any prevailing direction of magma propagation, because there is no general direction of the melt flow in the peripheral subsurface zones of large intrusions.

Keywords: anisotropy of magnetic susceptibility, Siberian traps, large sills, rock magnetism, Permian, Triassic

INTRODUCTION

The Siberian traps province is one of the vastest areas of Phanerozoic intraplate mafic magmatism, which could be considered as a reference example of a Large Igneous Province (LIP) (Coffin and Eldholm, 1994; Ernst, 2014). Moreover, the researchers' attention is likely to be drawn to the Siberian Traps becouse of the cause-and-effect connection of the disastrous extinction between the Permian and the Triassic when the intensive mafic magmatism resulted in trap rocks formation (Courtillot and Renne, 2003; Saunders and Reichow, 2009), and also with the largest copper-nickel and platinoid deposits in the Norilsk Region associating with layered trap intrusions.

Isotopic geochronological dating gives evidence of the fact that the most Siberian Traps formed for 1–2 Ma at Permian–Triassic boundary (Kamo et al., 2003; Reichow et al., 2009; Burgess and Bowring, 2015). However, some dates point at possible magmatism traces for the following period of 10–15 Ma (Ivanov et al., 2013).

Within the limits of the Siberian Platform, the Permian–Triassic Traps tend to form a vast field for the products of effusive and explosive magmatism. Several regions are distinguished which differ by the tectonic structure, composition and thickness of the volcanic sequence: Norilsk, Maimecha–Kotui, Putorana Plateau and Lower Tunguska (Fedorenko and Czamanske, 1997). On the periphery of the volcanic field, the trap formation is represented by thick and extensive dolerite sills intruding into the Paleozoic sedimentary cover deposits of the Siberian Platform.

In spite of prolonged investigations of the Siberian trap province, most issues of the genesis, mechanism and formation sequence of intrusive complexes have not been resolved yet. At present, the concept of mantle plumes (Campbell, 2005; Dobretsov et al., 2010) appears to be the most popular hypothesis explaining the origin of the intraplate basalt provinces including the Siberian Traps. However, alternative models have been proposed: lithosphere delamination (Elkins-Tanton, 2005), subduction (Ivanov, 2007), convective partial melting (King and Anderson, 1998) and a shear of the lithosphere (Czamanske et al., 1998). The present study is concerned with the problems of the trap intrusions formation to be discussed based on the plume hypothesis.

Despite the dominating assumption of mantle plume genesis of the Siberian trap rocks, a detailed scheme of the plume magmatism dynamics and evolution has still to be developed. The most common is the hypothesis of the plume center position under the Norilsk Region (Sobolev et al., 2011), where the volcanic sequence gains its maximum thickness and contains highly-magnesian lava from the Gudchikha and Tuklon Formations (Krivolutskaya, 2013).

✉ Corresponding author.
E-mail adress: anton.latyshev@gmail.com (A.V. Latyshev)

However, there exist alternative opinions. For instance, (Saunders et al., 2005) consider the plume head to be located in the territory of the West Siberian rift system.

The mechanisms of the magmatic melt transport to the Earth's crust are still unclear. Taking into account the gigantic dimensions of the Siberian Traps, significant lateral magma flows are supposed to have taken place due to extended sills which are exposed on the periphery of the Tunguska syneclise (Burgess et al., 2017). An important role of complex intrusions in the process of Large Igneous Province formation has been already demonstrated for other regions of mafic magmatism (Svensen et al., 2012; Magee et al., 2016).

The study presents the findings of detailed AMS investigations of intrusions within the Angara–Taseeva syneclise (southern periphery of the Siberian trap province) in order to reconstruct the directions of magma transport and to determine the position of main magma-feeding zones.

LITERATURE REVIEW OF AMS STUDIES AIMED AT RECONSTRUCTIONS OF MAGMA FLOW

A great number of studies are devoted to the anisotropy of magnetic susceptibility in igneous bodies (Khan, 1962; Knight and Walker, 1988; Ernst and Baragar, 1992; Raposo and Ernesto, 1995; Canon-Tapia, 2004). Most cited publications are concerned with reconstruction of magmatic flow directions in thin dikes based on orientation of the main axis of the AMS ellipsoid. The strengths of this methodology lie in the feasibility, so it can be applied for a wide range of igneous rocks without distinct oriented textures; to carry out high-speed measurements, to provide large-scale determinations for a quantity of samples.

The "normal" magnetic fabric (*N*-type) is considered to be the most common for planar intrusions (dikes and sills). It is the type of the magnetic fabric where the minimum K3 axis of the AMS ellipsoid is orthogonal to the contact, and the other two K1 and K2 axes lie in the plane of the intrusive body (Rochette et al., 1991; Tauxe et al., 1998). The usual practice is to interpret the orientation of the maximum K1 axis as the direction of the magmatic melt flow (Knight and Walker, 1988; Ernst and Baragar, 1992; Raposo and Ernesto, 1995). The distribution of the AMS ellipsoid axis is generally based on the dominating orientation of titanomagnetite and magnetite crystals, which appear to be widespread minerals in the rocks with such a composition (Raposo and Ernesto, 1995; Varga et al., 1998). Other mechanisms resulting in the normal-type ellipsoid are probably due to the contact friction arising at the time of emplacement and fracture closure caused by a decrease in magma pressure (Andersson et al., 2016). The distribution pattern of the AMS ellipsoid axis (where the maximum K1 axis is orthogonal to the intrusion plane) is called an inverse or reverse-type magnetic fabric (Rochette et al., 1999), and it is widespread in basic dike complexes (Rochette et al., 1999; Callot et al., 2001; Airoldi et al., 2012).

Different authors propose possible interpretation variants of the ellipsoid axes inversion, such as (1) domination of single-domain magnetite or maghemite grains among magnetic minerals (Potter and Stephenson, 1988); (2) crystal growth of magnetic minerals perpendicular to the contact (Hargraves et al., 1991; Cowan, 1999); (3) convection and gravitational particles deposition in subhorizontal tabular bodies (Rochette et al., 1999); (4) magnetostatic interaction (Hargraves et al., 1991; Borradaile and Jackson, 2010); (5) thermal contraction and formation of columnar jointing (Almquist et al., 2012; Hrouda et al., 2015); (6) postmagmatic deformations and metamorphism. The abovementioned interpretation variants do not reflect the whole diversity of versions offered to explain the phenomenon of "inverse" magnetic texture, but the universal solution has not been found yet. For most cases of inverse type-ellipsoid in intrusive bodies, authors avoid giving any interpretation of the magma flow direction.

If the intermediate K2 axis of the AMS ellipsoid is orthogonal to the intrusion contact, such a type of the magnetic fabric is referred to as intermediate (Park et al., 1988; Rochette et al., 1999). This distribution of ellipsoid axes inside dikes is interpreted as a result of vertical contraction during cooling and consolidation of a static magma column, provided the minimum K3 axis is vertical (Park et al., 1988; Raposo and Ernesto, 1995). There exist other ways of intermediate magnetic texture interpretation (*I*-type), for instance, combination of multi- and single-domain grains of magnetite or maghemite (Ferre et al., 2002); or overlapping of various factors forming anisotropy of magnetic susceptibility, for example, the magma flow and stress under conditions of intrusion cooling (Dragoni et al., 1997).

A number of studies deal with AMS investigation in lopoliths and sub-tabular intrusions, although they are not so numerous compared with dike investigations (Dragoni et al., 1997; Didenko et al., 1998; Cowan, 1999; Polteau et al., 2008; O'Driscoll et al., 2015). The magnetic fabric is estimated not only by the direction of the magma flow in thick tabular bodies. In addition, the magnetic fabric is determined by the processes of crystal deposition at cooling, crystallization *in situ*, postcumulus compression etc. (O'Driscoll et al., 2015). Consequently, the AMS of such bodies is studied not only for restoration of magma propagation, but also for reconstruction of structural and textural evolution of intrusions. However, similar to dikes, multiple examples of normal, reverse and intermediate magnetic fabric were recorded (Dragoni et al., 1997; Cowan, 1999; Ferre, 2002).

The AMS data are not commonly used for igneous complexes investigation in Russia, although the feasibility of application of this technique has been discussed in Russian geological literature long before (Sholpo, 1977; Sholpo et al., 1986). Even though some publications prove to be examples of appropriate and successful studies of the magnetic texture of basic intrusions (Didenko et al., 1998; Kurenkov et al., 2002; Konstantinov et al., 2014b), systematic AMS investigations of intrusions in most regions of the Siberian trap province and other LIPs are still not undertaken.

The present research objective is the detailed study of the anisotropy of magnetic susceptibility in the Angara–Taseeva depression intrusions (preferably in the sills) and reconstruction of main directions for the magmatic melt flow.

GEOLOGIC STRUCTURE AND SUBJECTS OF RESEARCH

The Angara–Taseeva syneclise is located in the southern part of the Siberian Platform, southwards the main field of vulcanic trap distribution (Fig. 1). Within the limits of the syneclise, the products of the Permian–Triassic magmatism are represented by thick and extensive dolerite sills and tuffs from the Korvunchan (Kapaevo) Formation. The sills are intruding into the Paleozoic sedimentary cover deposits of the Siberian Platform. They are distinguished by thicknesses of 200–300 m and huge expansion areas (Feoktistov, 1978). Based on field observations and well data analysis, no less than 6 large intrusions have been identified at different levels of the Paleozoic deposits: the Usol'e, Zayarskii, Tulun, Tolstyi Mys, Padun and Chuna–Biryusa sills (Feoktistov, 1978; Ivanov et al., 2013; Latyshev et al., 2013).

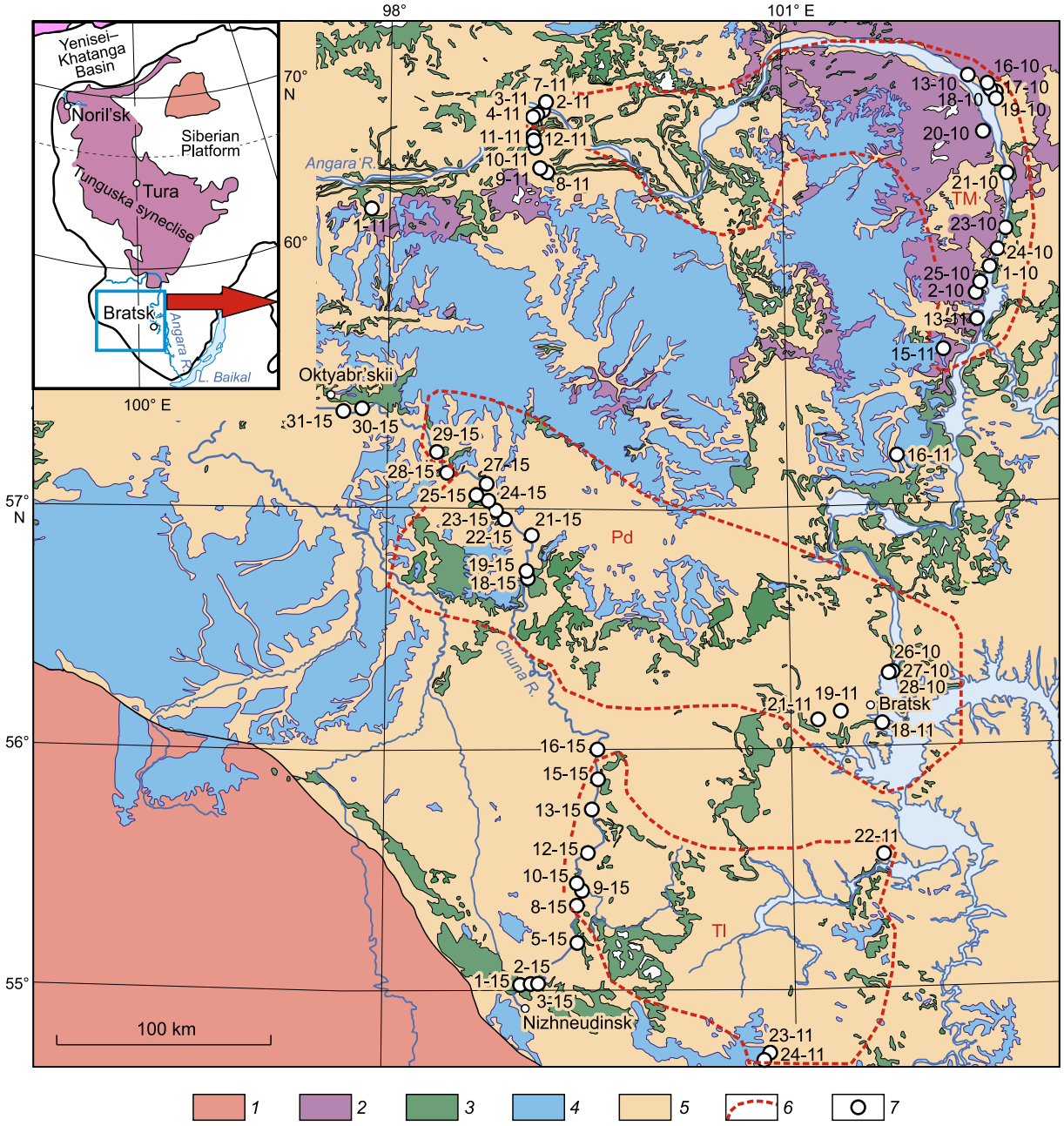

Fig. 1. The geology of the investigated area. *1,* Precambrian; *2*, *3*, Permian–Triassic Traps: *2*, lava and tuffs, *3*, intrusions; *4*, Jurassic; *5*, Paleozoic deposits of the Siberian Platform; *6*, boundaries of large sills; *7*, the sampling location of oriented specimens. Large dolerite sills: Pd, Padun, Tl, Tulun, TM, Tolstyi Mys.

Nevertheless, it is quite a challenging task to set the boundaries of the intrusive bodies using field data. All of the sills tend to localize at higher stratigraphic levels trending from the west to the east. Consequently, magma intrusion supposedly propagated from the west to the east within the borders of the Angara–Taseeva syneclise, and the magma-feeding zone lay in the central, most downwarped part of the current depression (Feoktistov, 1976).

Tuffaceous deposits (from the Korvunchan (Domyshev, 1974) and Kapaevo (Naumov and Ankudimova, 1995) formations) together with associated breccia pipes are also found within the Angara–Taseeva syneclise. The iron-ore deposit of Angara–Ilim district is assigned to these breccia pipes, which are known to be vents for large intrusions (Naumov and Ankudimova, 1995; Svensen et al., 2009; Fristad et al., 2017).

The sills' age is determined by numerous modern U–Pb and $^{40}Ar/^{39}Ar$ dating (Ivanov et al., 2005, 2009, 2013; Paton et al., 2010; Burgess and Bowring, 2015). Two age-groups have been distinguished: 252–249 Ma (Late Permian–beginning of the Early Triassic) and 243–239 Ma (Middle Triassic). Some age determinations are contradictory although they are obtained by different methods for the same bodies (Latyshev et al., 2013, 2018), and most issues concerning the age of particular intrusions and magmatism duration are still unresolved. We consider the ages of the Padun and Tolstyi Mys sills to be the most appropriate. According to U–Pb zircon dating their age is about 251 Ma, which corresponds to the Permian–Triassic boundary (Paton et al., 2010; Burgess and Bowring, 2015).

The subjects of the present study are intrusive bodies, which are found within the Angara–Taseeva syneclise in the Angara and Chuna valleys. We have investigated 65 sites; the sites are mainly represented by sills (60 sites) and rarely by dikes and intrusions with indistinct morphology (5 sites); no less than 5 oriented specimens from each site. The sills and dikes are dominated by dolerites and gabbro-dolerites. They are up to 200–250 m thick and form concordant bodies inside the Paleozoic sedimentary cover of the Siberian Platform, but in the northeast the depressions intrude even through the Triassic tuffaceous deposits. Paleomagnetic investigations allowed us to determine that intrusive bodies had formed during three great but short magmatic events, which were responsible for the emplacement of the Tulun, Padun and Tolstyi Mys sills and associated small subvolcanic bodies. Moreover, less extensive episodes of magmatism resulted in formation of separate relatively small intrusions. The duration of emplacement of these magmatic events were also determined. The details of paleomagnetic investigations are given in (Latyshev et al., 2013, 2018) and will be omitted in the present discussion.

RESEARCH METHOD

The AMS measurements were carried out with the use of an MFK-1FA kappa-bridge (AGICO) at the laboratory of Main geomagnetic field and rock-magnetism at Schmidt Institute of Physics of the Earth, Russian Academy of Sciences, Moscow. The Anisoft 4.2 software was used for measurements processing based on the statistical techniques described in (Jelínek and Kropáček, 1978). To analyze the AMS ellipsoid, P_j (corrected degree of anisotropy) and T (ellipsoid shape) parameters were used. The degree of anisotropy was calculated by formula:

$$P_j = \exp\left(\sqrt{2\times(n1-n)^2 + ((n2-n)^2 + (n3-n)^2)}\right),$$

where

$$n1 = \ln(\mathrm{K1}); \quad n2 = \ln(\mathrm{K2});$$

$$n3 = \ln(\mathrm{K3}); \quad n = \sqrt[3]{n1\times n2\times n3},$$

K1, K2, K3 denote the maximum, intermediate and minimum main axes of the AMS ellipsoid, respectively (Jelínek, 1981).

The ellipsoid shape parameter T was calculated by the formula:

$$\mathrm{T} = \left(2\times\ln(\mathrm{K2}) - \ln(\mathrm{K1}) - \ln(\mathrm{K3})\right) / \left(\ln(\mathrm{K1}) - \ln(\mathrm{K3})\right).$$

The temperature curves of magnetic susceptibility were measured in the field of 0.4 T using the Curie balance designed by Yu.K. Vinogradov. Hysteresis loops were obtained with a PMC MicroMag 3900 vibromagnetometer at room temperature and in 0.5 T saturation field. The domain structure of ferromagnetic grains was determined by the Day-Dunlop diagram (Day et al., 1977; Dunlop, 2002). Anisotropy of anhysteretic (ideal) remanent magnetization (AARM) was measured using a JR-6 (AGICO) spin-magnetometer and an LDA-3A system of alternating-field demagnetization fitted with an AMU-1A (AGICO) attachment of anhysteresis magnetization. The measurements were conducted at the Laboratory of Applied Methods of Geodynamic Studies, at the Department of Geology of Lomonosov Moscow State University.

STRUCTURAL AND PETROGRAPHIC DATA

The morphology of tabular igneous bodies is one of the possible information sources of the flow direction; that is of prime concern for reconstructing propagation of the magma flow. Intrusive steps, bridge structures and magma lobes are known to be as mesostructure-indicators in intrusive bodies. In the general case, the long axis is interpreted as the melt flow direction for all these structural elements (Schofield et al., 2012; Magee et al., 2016; Hoyer and Watkeys, 2017). Such an interpretation is based on the supposition that the initial magma intrusion takes place along the series of parallel laterally limited canals, which are separated from each other by the screens of host rock. Then at further magma inflation, these segments merge together forming a singular

tabular body, and the places of "stoppings" are marked with steps or remnants of host rocks.

Unfortunately, constrained exposure prevents from conducting a complete structural analysis of the sills from the Angara–Taseeva depression. In the center of the studied region, the most part of exposed contacts of the intrusive bodies is represented by smooth surfaces without apophyses, steps and other structures indicating the direction of magma flow. Site 15-15 is the exception, where the exposed contact of the Tulun sill with the Ordovician terrigenous deposits from the Bratsk Formation was found on a cliff on the Chuna River (Fig. 2*A*). The outcrop of the intrusive flat-lying body is trending in the NW direction. On the contrary, the contact is in shape of a subvertical step, which is 3 meters high and has an apophysis forming the concordant body with the host rocks. Host sandstones and siltstones of the exocontact zone are shallowly dipping, deformed and shifted with small-amplitude reverse faults during the emplacement of sill. The contact is trending in the NW direction (azimuth 330). In case such closing of a sill is interpreted as the intrusion step, we come to the conclusion that the magma transport could have been parallel to the subvertical part of the contact, that is, in the NW–SE direction.

Thin sills and multidirectional dikes are mostly dominating in the Angara valley on the eastern periphery of the Angara–Taseeva syneclise in comparison with the inner part of the depression. It indirectly points at the absence of the common direction of the magma flow in this region. Moreover, localization of most intrusive bodies in the Lower Triassic tuffs of the Korvunchan Formation is indicative of emplacement at shallow depth.

Orientation analysis of the long axes of rock-forming mineral grains could be considered as another possible restoration method of magma flow direction. Petrographic studies of thin rock sections demonstrated that most of the sampled intrusive bodies were composed of dolerites with poikilitic and poikilophitic texture. About 90–95% of the rock volume is dominated in the whole by basic plagioclase (labradorite) and clinopyroxene; herewith, large oikocrysts of clinopyroxene contain small elongated chadacrysts of plagioclase (Fig. 2*B*). Olivine and titanomagnetite occur in subordinate quantities (to 10%). The crystal size and rock structure vary depending on the thickness of the body and its position inside the intrusion. Near-contact zones are often comprised of gabbro-porphyrites and even of versicular basalts (Fig. 2*B*); the thickness of the versicular zone in the

Fig. 2. Results of structural and petrographic studies. *A,* photo of site 15-15, the Tulun sill contact with Ordovician deposits from the Bratsk Formation labeled with a dashed line; *B*, *C*, photo of rock thin section in crossed-polarized light: *B*, dolerite, site 22-15, the Padun sill, *C*, versicular basalt, site 31-15, endocontact sill zone. Pl, plagioclase, Cpx, clinopyroxene.

upper part of separate sills reaches 2 m. Regular orientation of crystals, which could be interpreted as the result of the melt flow, has not been detected in all rock thin sections.

RESULTS OF MAGNETIC ANISOTROPY STUDIES

The sampled rocks from most studied sites showed a low anisotropy degree of magnetic susceptibility (AMS)—P_j < 1.04, and only in rare cases it increased up to 1.06 (Fig. 3*A*). Such values of the P_j parameter are typical of basites with a magnetic fabric of primary magmatic genesis (Tarling and Hrouda, 1993).

The values of the T parameter characterizing the shape of the AMS ellipsoid (Jelínek, 1981) varied from –0.5 to 0.5 for most sites; herewith, the ellipsoid had a prolate form (T > 0) in ≈50% of cases, but it was oblate (T < 0) for the rest 50% of cases. As a rule, the prolate form of the AMS ellipsoid in igneous bodies is interpreted as a result of the magma flow; while the oblate form is a result of static processes in the bodies such as compression or cooling, crystallization *in situ* or gravitational differentiation (O'Driscoll et al., 2015; Andersson et al., 2016). No apparent dependence of the T value on the degree of anisotropy P_j was found (Fig. 3*A*). Low values of the anisotropy degree and variations in the ellipsoid shape indicate that the studied intrusive rocks possess an igneous magnetic fabric, whose formation was due to several factors such as propagation of the magmatic melt, local stresses related to cooling of the body (Tarling and Hrouda, 1993; Andersson et al., 2016) and also to crystallization deposition of magnetic particles (O'Driscoll et al., 2015).

The distribution analysis of the AMS ellipsoid axis in relation to the intrusion contacts has shown that 32 sites from 65 (49%) are characterized by normal type magnetic fabric (ellipsoid axis orientation and anisotropy parameters values per site are given in a table in the supplement). These sites, with minor exceptions, belong to sills with subhorizontal contacts, and the minimum ellipsoid K3 axis is oriented perpendicular to the contact, i.e., subvertically. The remaining two K1 and K2 axes have a flat orientation and almost lie in the intrusion plane. Being statistically different from other axes, the directions of the maximum K1 axis are tightly grouped in 16 sites (Fig. 3*B*). In the remaining cases they form a great-circle arc with the directions of the intermediate K2 axis (Fig. 3*C*). Imbrication of the K1 axis from the horizontal plane is commonly negligible, but in some cases, it reaches 20°, that could have been caused by a turbulent magma flow. Orientation of the K1 axis at the sites with a normal-type AMS ellipsoid is interpreted as being consistent (within confidence intervals) with the magma flow direction.

An inverse type of the magnetic fabric with the maximum K1 axis was recorded at 14 sites (22%). Here, the maximum K1 axis is oriented perpendicular to the contact and subvertically in the sills. Thus, the K2 and K3 axes are oriented horizontally and lie in the plane of intrusion (Fig. 3*D*). The reasons of the magnetic fabric inversion will be discussed below.

Across the remaining 19 sites (29%), we determined either an intermediate fabric with the central K2 axis being orthogonal to the contact (Fig. 3*E*), or diagonal to the intrusion contacts, or chaotic axis distribution inside the site. The results from these sites were not applied for further interpretation. It should be noted that the part of the sites with chaotically oriented axis of the AMS ellipsoid is distinguished by a rather low degree of anisotropy—P_j < 1.01, that might predetermine the absence of the regular magnetic fabric.

ROCK-MAGNETIC PROPERTIES

The curves of thermomagnetic behavior (obtained up to 650 °C) indicate that magnetite or low-titanium titanomagnetite with Curie points from 450 to 580 °C appear to be essential magnetic minerals in most of the studied dolerite samples. Figure 4 presents the typical curves of thermomagnetic behavior, which correspond to nearly pure magnetite at T_c = 550 °C (*A*) or to titanomagnetite at T_c = 480 °C (*B*). Such mineral composition of the magnetic fraction is typical for Siberian trap rocks and has been frequently determined both for lava facies (Heunemann et al., 2004) and for intrusions (Konstantinov et al., 2014a; Shcherbakov et al., 2017). At the same time, the sites with the "normal" or "reverse" magnetic texture display no regular differences both by thermal curves and via stepwise thermal cleaning.

The values of hysteresis parameters for M_{rs}/M_s and H_{cr}/H_c samples vary in the ranges of 0.05–0.3 and 1.5–3.5, respectively; according to the Day-Dunlop diagram (Day et al., 1977; Dunlop, 2002), all the samples get into the field of pseudo-single-domain grains (Fig. 4*C*). It should be noted that the samples from the sites with both normal and reverse types of the AMS ellipsoid tend to be close to the curve corresponding to mixing of single-domain and multidomain grains (Dunlop, 2002), but the former are more biased towards "single-domain field". This fact contradicts the most common explanation of the inverse-type magnetic fabric occurrence mainly based on single-domain composition of magnetite grains (Potter and Stephenson, 1988; Tarling and Hrouda, 1993; Cagnoli and Tarling, 1997; Rochette et al., 1999). At the same time, two clusters can be identified for the *R*-type samples, whose position is correlated with the thickness of intrusion and the grains size of the magnetic minerals. The samples with ratios M_{rs}/M_s < 0.1 and H_{cr}/H_c = 2.8–3.5 are much closer to the multidomain field, and mostly represent coarse-grained internal zones of large sills. However, the samples with ratios M_{rs}/M_s = 0.1–0.2 and H_{cr}/H_c = 1.7–2.2 are not different from the samples of *N*-type by these parameters; as a rule, they usually represent thin bodies or near-contact zones of large sills.

Anisotropy of anhysteretic remanent magnetization (AARM) was measured in 8 samples with the *R*-type AMS

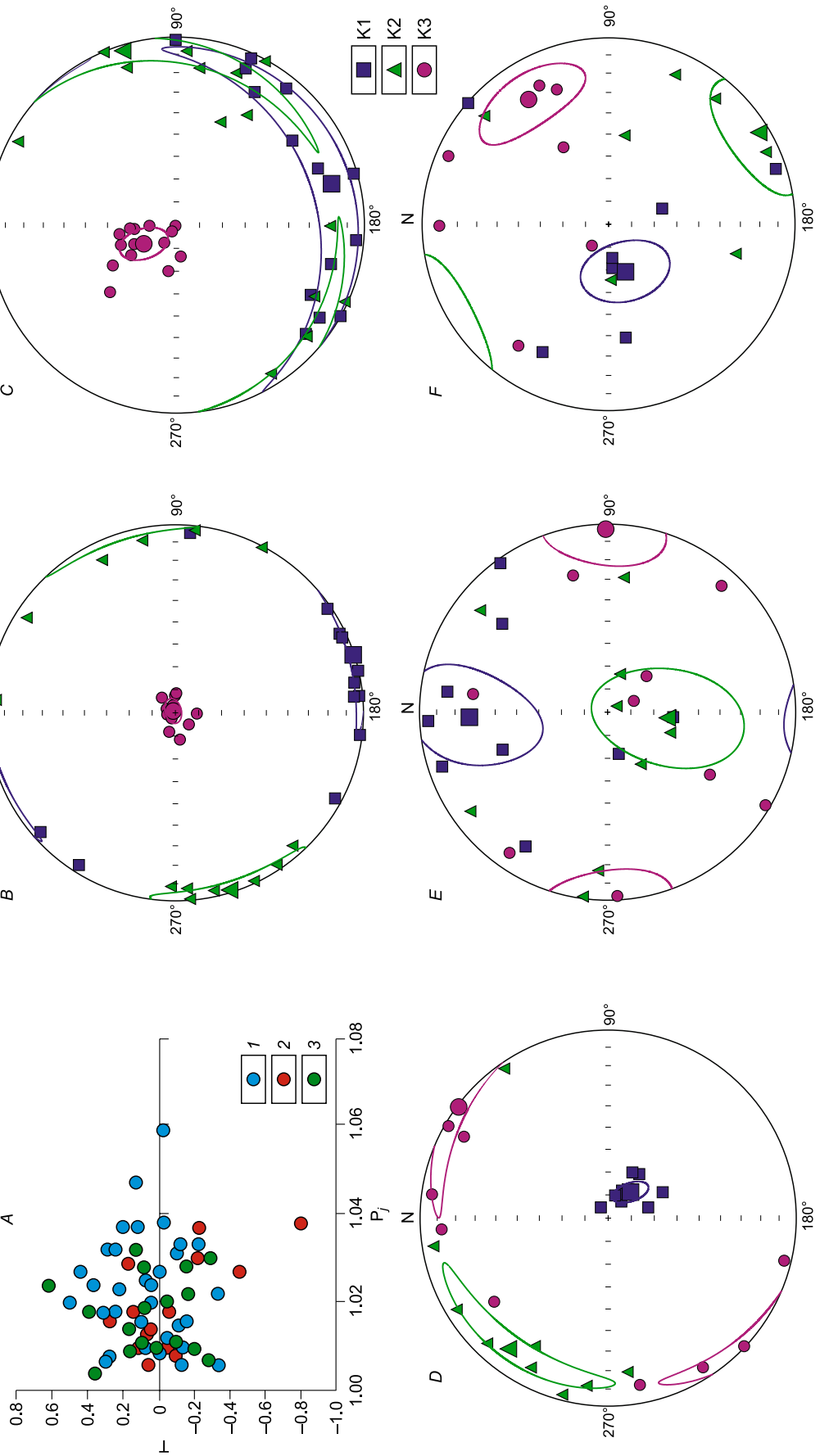

Fig. 3. Measurements of anisotropy of magnetic susceptibility (AMS). *A*, the Jelínek diagram (Jelínek, 1981): T, an ellipsoid shape parameter; P_j, anisotropy degree, *1*, sites with a *N*-type AMS ellipsoid; *2*, sites with *R*-type magnetic fabric; *3*, sites with intermediate, diagonal and chaotic types; *B–F*, AMS ellipsoid examples. Stereographic equal-area projection, lower hemisphere. K1, maximum axis; K2, intermediate axis; K3, minimum axis. *B*, site 10-15, *N*-type; *C*, site 12-15, *N*-type; *D*, site 18-15, *R*-type; *E*, site 21-15, intermediate type; *F*, site 13-15, dike, *N*-type.

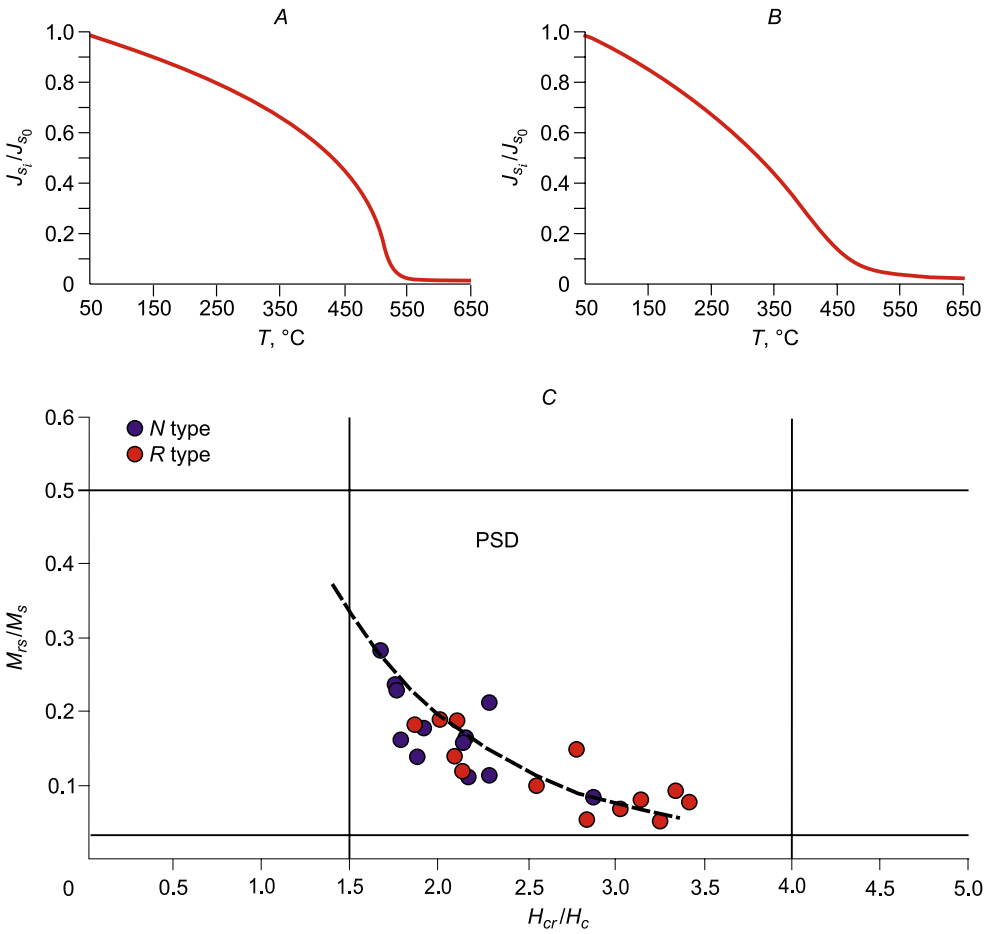

Fig. 4. Rock magnetic properties. *A*, *B*, thermal curves $J_s(T)$. J_{s_i}, saturation magnetization; Js_0, saturation magnetization at room temperature. *A*, sample 103, site 8-15, *N*-type; *B*, sample 309, site 20-15, *R*-type; *C,* the Day-Dunlop diagram (Day et al., 1977; Dunlop, 2002). M_s, saturation magnetization; M_{rs}, remanent saturation magnetization; H_c, coercive force; H_{cr}, remanent coercive force. PSD, field of pseudo-single-domain grains. The dashed line—mixing of single-domain and multidomain grains (Dunlop, 2002).

ellipsoid (Table 1). Since AARM does not depend on the domain composition (Potter and Stephenson, 1988), in case of significant contribution of single-domain grains in AMS inversion we will expect the maximum and minimum axis to change their position when AMS and AARM are compared; in other words, AARM will demonstrate *N*-type anisotropy.

In our case, orientations of mean axes for AMS and AARM ellipsoids are found to be close to each other. Thus, it does not confirm the version of single-domain composition of the magnetic grains in *R*-type samples: in both cases, K1 underlies steeply, K2 and K3 are oriented horizontally (Fig. 5). Nevertheless, the AARM (Fig. 4*A*) estimates demonstrate greater variance in comparison with AMS (Fig. 4*B*), and the position of the ellipsoid axes can greatly and sometimes radically differ for some speciments (Table 1). Therefore, comparison of AMS and AARM measurements confirms the insufficiency of difference in domain composition to explain well-manifested inversion of maximum/minimum axes of the AMS ellipsoid. Consequently, supportive studies must still be conducted for complete interpretation of differences in axes orientation in separate samples.

DISCUSSION

The findings of rock-magnetic investigations give evidence of the fact that the inversion of the AMS ellipsoid in the dolerite samples cannot be explained by differences of magneto-mineralogical and domain composition. Since the studied igneous bodies lie within the limits of the Siberian Platform region, which was not subjected to significant tectonic deformations and endogenous activities after Triassic, the version of postmagmatic variations in the magnetic fabric is unlikely to be probable. At present, by way of illustration of possible “inversion” mechanisms let us consider: thermal contraction through forming of the columnar jointing (Almquist et al., 2012), which is well-represented in the studied embedded intrusions; crystallization in stationary magma (Tauxe et al., 1998), and gravitational particles deposition under crystallization differentiation in thick sills (Rochette et al., 1999). The last version explains *R*-type samples proximity to the multidomain field on the Day-Dunlop diagram. Nevertheless, to receive the ultimate answer to this question, detailed rock magnetic studies of con-

Table 1. AARM measurements and their comparison with AMS in *R*-type samples

Sample	Site	AARM						AMS					
		K1		K2		K3		K1		K2		K3	
		D	I	D	I	D	I	D	I	D	I	D	I
287	18-15	107.4	50.5	204.5	5.8	299.2	38.9	107.1	79.7	328.5	7.7	237.6	6.7
3	1-15	355.4	88.0	214.0	1.5	123.9	1.2	333.5	82.3	209.1	4.4	118.6	6.3
311	20-15	309.8	17.4	47.6	23.4	186.8	60.2	173.3	78.1	307.7	8.4	39.0	8.4
313	20-15	75.2	42.9	315.0	28.4	203.7	33.9	15.0	87.5	234.9	1.9	144.9	1.6
314	20-15	147.1	57.1	320.1	32.7	52.1	3.2	125.0	61.7	294.4	27.9	26.8	4.4
315	20-15	8.5	48.4	270.3	7.2	174.0	40.7	283.7	86.5	121.5	3.3	31.4	1.1
316	20-15	102.2	9.8	325.4	76.6	193.8	9.0	100.5	55.7	292.5	33.7	198.7	5.6
6	1-15	60.2	61.6	288.5	19.8	191.1	19.5	112.2	50.6	242.9	28.2	347.4	25.1

Note. AARM, anisotropy of anhysteretic remanent magnetization; AMS, anisotropy of magnetic susceptibility; K1, maximum ellipsoid axis; K2, intermediate axis; K3, minimum axis; *D*, declination, deg.; *I*, inclination, deg.

crete igneous bodies with the expressed inversion of the AMS ellipsoid have to be conducted.

To reconstruct the directions of the magma flow, we used the directions of the maximum axis of the AMS ellipsoid with a normal-type of magnetic fabric (30 sites). Figure 6 presents K1 axis orientations at the sites with normal and reverse types of the ellipsoid and shows that the *N*-type magnetic fabric with the flatly-oriented maximum ellipsoid axis in the sills tends to dominate in the Chuna Valley, i.e., in the region lying in the vicinity of the central part of the Angara–Taseeva syneclise. At the same time, *R*-type sites are predominant on the periphery of the depression in the Angara valley.

Previous paleomagnetic investigations let us conclude that the Chuna River intrusions form several compact clusters, or directional groups with apparently different paleomagnetic directions (Latyshev et al., 2018). These groups correspond to discrete episodes of magmatism related to emplacement of large sills or series of intrusions. Several groups of sites are distinguishable among sampled locations in the Chuna valley; they are: 18-15–29-15 (Padun sill), 8-15–15-15 (Tulun sill) and 1-15–5-15 (Nizhnyaya Uda sill). Distribution of maximum axes of the AMS ellipsoid inside different groups allows finding definite regularities. For instance, K1 axis orientations in the *N*-type sites (relate to the Padun sill) are forming a fan converging to the southwest, i.e., towards the most downwarped part of the Angara–Taseeva depression in the Biryusa valley. SW and NE K1 axis dips are both observed, although dip angles does not exceed 20°. The change in the direction of the gently dip-

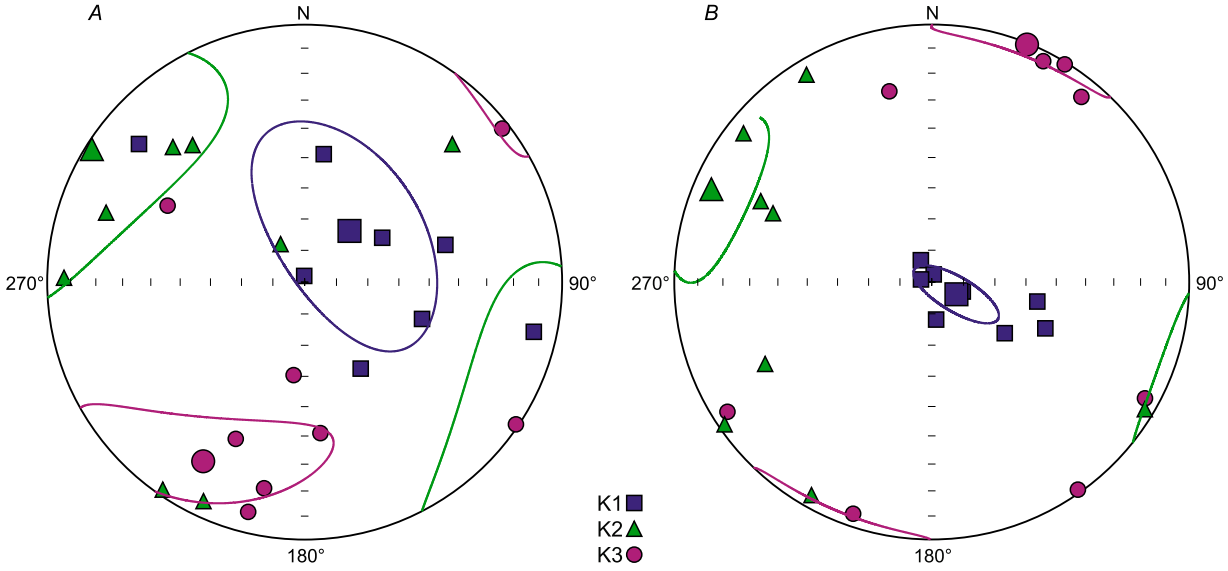

Fig. 5. Measurements of anisotropy of anhysteretic remanent magnetization (AARM) of *R*-type samples; comparison with AMS of the same samples. Stereographic equal-area projection, lower hemisphere. K1, maximum axis; K2, intermediate axis; K3, minimum ellipsoid axis. *A*, measurements of AARM; *B*, measurements of AMS.

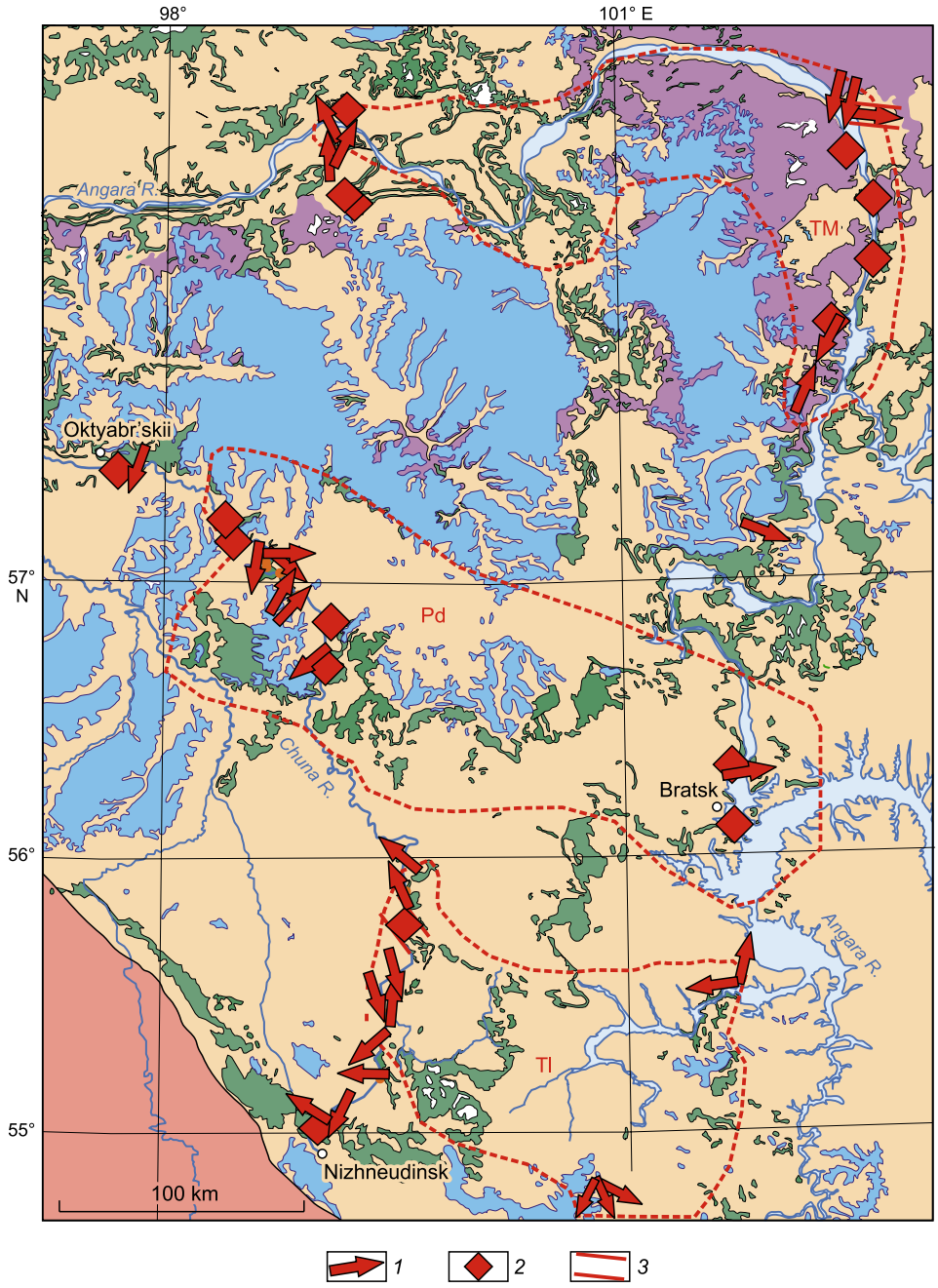

Fig. 6. Distribution of orientations for the AMS ellipsoid maximum axes at sites with *N*- and *R*-type magnetic fabric. *1*, dip direction of the maximum axis at *N*-type sites (gently plunging K1 direction); *2*, steep plunge of K1 axis (*R*-type); *3*, strike of dike contacts. For the rest conventional signs see Fig. 1.

ping maximum axis could be explained by an measurement error or by deflection of the magma flow from the horizontal plane. The fan-like turn of the K1 axis orientations and their SW convergence agree with the hypothesis of the sill propagation from the central part of the depression (Feoktistov, 1978). At the same time, we should point at the occurrence the adjacent sites with lateral orientations of the K1 axis, which do not fit the general pattern, and at a number of sites with the *R*-type magnetic fabric. The occurrence of lateral orientations across the general direction of the maximum axis orientation could be due to the sites location directly on intrusion steps or "bridges" connecting separate segments of the a large sill. The melt flow is often oriented laterally across the intrusion direction in these structures (Hoyer and Watkeys, 2017). However, the lack of structural data prevents an unambiguous interpretation.

The NNW orientations of K1 axis are predominant at the sites belonging to the Tulunsk sill group with the exception of site 8-15, which is close to the Nizhnyaya Uda sill (see below). Moreover, the dike (site 13-15) extending north-

westward also belongs to this group, and the K1 axis (enclosed in the dike) is characterized by steep orientations (Fig. 3*F* and Supplement (http://sibran.ru/upload/medialibrary/d60/d60946ebbae459110d9a31d8fa224f8b.pdf)). The character of the intrusion magnetic fabric complies with the melt flow in the SE direction along a local weak zone. This interpretation is consistent with the structural data on site 15-15, where NW–SE emplacement direction (azimuth 330) is reconstructed by the orientation of the intrusive step contact. At this site, the maximum axis of the AMS ellipsoid gently plunges to the NW (azimuth 336) at a distance of 20 m from the contact, but the K1 axis is steeply oriented directly in the zone of the subvertical endocontact. Consequently, the direction of the sill emplacement reconstructed by structural and rock magnetic data is identical within confidence interval.

The Nizhnyaya Uda sill and closely spaced site 8-15 demonstrate convergence of the ellipsoid maximum axes towards the local center positioned to the west from the Chuna River in proximity to the Siberian Platform border. Therefore, all the studied groups of intrusive bodies in the Chuna valley are characterized by different dominating directions of the melt propagation and local magma-feeding centers. The sites with the *R*-type magnetic fabric are the most common in the area of the Tolstyi Mys and Padun sills in the Angara valley; but the maximum axis has a submeridional orientation at the sites with a normal-type ellipsoid. The *N*-type magnetic fabric dominates in the area of the Tulun sill, although the directions of the maximum K1 axis change sharply even at the adjacent sites (22-11–24-11; Figs. 1, 6). Significant extension of the *R*-type magnetic fabric in intrusions from the Angara valley could be related to the fact that only peripheral near-surface parts of the sills are exposed in these regions. For instance, the Tolstyi Mys sill and associated intrusions extending from Ust'-Ilimsk to the Kata River intruded into the Triassic tuffaceous deposits (almost of the same age) from the Korvunchan Formation (Naumov and Ankudimova, 1995; Latyshev et al., 2013). Approaching the closure parts of intrusions, the magma flow has a minor effect on the magnetic fabric, which is controlled by thermal contraction under cooling, gravitational deposition during differentiation that finally predetermines the observed *R*-type of the ellipsoid. Near-surface depths of the intrusions formation in the Angara valley are evidenced by more frequent occurrence (in comparison with the Chuna) of thin sills series (sites 13-10, 22-11) and multidirectional dikes with complex morphology (site 19-10), characterized by different emplacement modes. This could be assigned to the difference in orientations of K1 axes from the adjacent sites within the limits of the Tulun sill (22-11–24-11).

The obtained results are primarily important for searching the mechanisms of lateral magma transport during LIP formation. With regard to the Angara–Taseeva depression, most researchers hold the viewpoint that the thick sills of this region appear to be gigantic sheets or tabular bodies covering hundreds of kilometers, tending to extend from the center of the depression to its periphery and to intrude steadily at higher stratigraphic levels (Fig. 7*A*). The same structure of syneclise intrusive bodies is presented in almost all the studies describing schematic sections across depression (Feoktistov et al., 1978; Ivanov et al., 2013; Latyshev et al., 2013; Fristad et al., 2017). However, close mapping and seismic data on intrusive complexes from other igneous provinces give evidence of domination of small saucer-shaped subtabular bodies (Fig. 7*B*, *C*). The same data were obtained on sills from the Karoo Province (Galerne et al., 2008), the passive margin of the North Atlantic (Polteau et al., 2008, Magee et al., 2016) and the shelf of the Barents Sea (Polteau et al., 2016). Formation of tabular intrusion complexes is restricted either to vertical magma flow from separate deep magma chambers for each sill (Fig. 7*B*, (Malte-Sørenssen et al., 2004)), or to the magma transport from a singular chamber with extensive lateral melt propagation in the upper crust across the system of saucer-shaped sills and sloping "steps" (Fig. 7*C*, (Cartwright and Hansen, 2006). According to the proposed model and the data obtained on the Earth's LIPs, it should be noted that separate sills are not more than 60 km in diameter (intrusions of the Karoo Province (Polteau et al., 2008)), therefore the hypothetic sill length up to hundreds of kilometers is still left unexplained.

Unfortunately, discontinuous exposure of the sills within the Angara–Taseeva depression prevents us from tracing and determining if the groups of coeval intrusions separated by 200–250 km turn out to be the parts of a single gigantic sill. Nevertheless, the defined features of the magnetic fabric (fan-like turn of orientations for the maximum axis of the AMS ellipsoid and the axes convergence at the local centers) is evidence of a series of separate intrusive bodies. Moreover, the occurrence of directional groups with close paleomagnetic directions in the center and on the periphery of the depression (Latyshev et al., 2018) points at synchronous emplacement of such intrusions in different parts of the province.

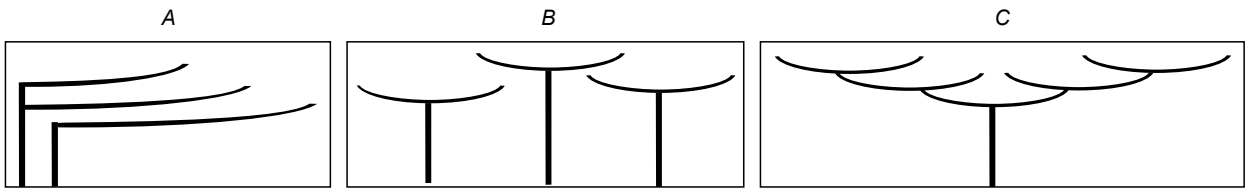

Fig. 7. Model of large sills intrusion from the Angara–Taseeva depression. *A*, gigantic tabular bodies intruding from the common feeding zone (Feoktistov, 1978; Ivanov et al., 2013); *B,* model of multiple deep magma chambers (Malte-Sørenssen et al., 2004; Galerne et al., 2008); *C*, model of a single deep magma chamber and lateral propagation via the sill system (Cartwright and Hansen, 2006; Galerne et al., 2008).

At present, we cannot make a choice between the models presented in Fig. 7*B, C* because of insufficient information. Based on geochemical differences over the sills of the Golden Valley complex (Karoo Province), the study (Galerne et al., 2008) supposes the melt to flow from several isolated mantle sources. Published geochemical data on the Tulun, Padun and Tolstyi Mys sills (Ivanov et al., 2009, 2013) indicates that they originated from a single source and their affinity with low-potassium, low-Ti, and tholeiitic basalts which make up the bulk of the traps of the Siberian Platform (Fedorenko et al., 1996). Furthermore, the cited publications present only fragmentary data on the sills of the Angara–Taseeva syneclise, consequently, systematic geochemical survey should be done to find the ultimate answer to the question posed.

CONCLUSIONS

(1) Detailed investigations of the anisotropy of magnetic susceptibility in large dolerite sills of the Angara–Taseeva syneclise have revealed that only 50% of the studied sites have the normal-type magnetic fabric suitable for reconstruction of the magma flow direction.

(2) Intrusions with the normal-type magnetic fabric dominate in the central part of the syneclise (the Chuna valley). The maximum axes distribution of the AMS ellipsoid is different in large sills and points at the existence of local intrusion centers. The obtained results are generally consistent with the hypothesis of the magma-feeding zone position in the central, most downwarped part of the Angara–Taseeva depression.

(3) Intrusions with an AMS ellipsoid of a "reverse" type are predominant on the periphery of the depression. The direction of the magma flow is reconstructed by the adjacent sites, but it differs considerably across the area. That is explained not only by the absence of the general direction of the melt flow in the peripheral subsurface zones of large intrusions. The difference is also due to wide-spread occurrence of small hypabyssal and subvolcanic bodies with complex morphology and with various mechanisms and directions of emplacement.

The research was supported by the RFBR (grant 16-35-60114, 17-05-01121), and by the Government of the Russian Federation (grant 14.Z50.31.0017).

The authors wish to express their gratitude to E.M. Mirsayanova and D.A. Soboleva for their assistance in conducting the petromagnetic investigations. The authors also want to thank the reviewers for valuable comments and fair points which helped to improve the manuscript.

REFERENCES

Airoldi, G., Muirhead, J.D., Zanella, E., White, J.D.L., 2012. Emplacement process of Ferrar Dolerite sheets at Allan Hills (South Victoria Land, Antarctica) inferred from magnetic fabric. Geophys. J. Int. 188 (3), 1046–1060.

Almqvist, B.S.G., Bosshard, S.A., Hirt, A.M., Mattsson, H.B., Hetenyi, G., 2012. Internal flow structures in columnar jointed basalt from Hreppholar, Iceland: II. Magnetic anisotropy and rock magnetic properties. Bull. Volcanol. 74, 1667–1681. DOI 10.1007/s00445-012-0622-0.

Andersson, M., Almquist, B.S.G., Burchardt, S., Troll, V.R., Malehmir, A., Snowball, I., Kubler, L., 2016. Magma transport in sheet intrusions of the Alnö carbonatite complex, central Sweden. Sci. Rep. 6, 27635. DOI: 10.1038/srep27635.

Borradaile, G.J., Jackson M., 2010. Structural geology, petrofabrics and magnetic fabric (AMS, AARM, AIRM). J. Struct. Geol. 32 (10), 1519–1551.

Burgess, S.D., Bowring, S.A., 2015. High-precision geochronology confirms voluminous magmatism before, during, and after Earth's most severe extinction. Sci. Adv. 1 (7), e1500470. DOI: 10.1126/sciadv.1500470.

Burgess, S.D., Muirhead, J.D., Bowring, S.A., 2017. Initial pulse of Siberian Traps sills as the trigger of the end-Permian mass extinction. Nature Commun. 8 (164), 1–6. DOI: 10.1038/s41467-017-00083-9.

Cagnoli, B., Tarling, D.H., 1997. The reliability of anisotropy of magnetic susceptibility (AMS) data as flow direction indicators in friable base surge and ignimbrite deposits: Italian examples. J. Volcanol. Geotherm. Res. 75 (3–4), 309–320.

Callot, J.P., Geoffroy, L., Aubourg, C., Pozzi, J.P., Mege, D., 2001. Magma flow directions of shallow dykes from the East Greenland volcanic margin inferred from magnetic fabric studies. Tectonophysics 335 (3–4), 313–329.

Campbell, I.H., 2005. Large igneous provinces and the mantle plume hypothesis. Elements 1, 265–269.

Canon-Tapia, E., 2004. Anisotropy of magnetic susceptibility of lava flows and dykes: A historical account. Geol. Soc. London, Spec. Publ. 238, 205–225.

Cartwright, J., Hansen, D.M., 2006. Magma transport through the crust via interconnected sill complexes. Geology 34 (11), 929–932. DOI: 10.1130/G22758A.1.

Coffin, M.F., Eldholm, O., 1994. Large igneous provinces: crustal structure, dimensions and external consequences. Rev. Geophys. 32 (1), 1–36.

Courtillot, V.E., Renne, P.R., 2003. On the ages of flood basalt events. Geoscience 335 (1), 113–140.

Cowan, E.J., 1999. Magnetic fabric constraints on the initial geometry of the Sudbury Igneous Complex: a folded sheet or a basin-shaped igneous body? Tectonophysics 307 (1–2), 135–162.

Czamanske, G.K., Gurevich, A.B., Fedorenko, V., Simonov, O., 1998. Demise of the Siberian plume: paleogeographic and paleotectonic reconstruction from the prevolcanic and volcanic records, North-Central Siberia. Int. Geol. Rev. 40 (2), 95–115.

Day, R., Fuller, M., Schmidt, V.A., 1977. Hysteresis properties of titanomagnetites: Grain-size and compositional dependence. Phys. Earth Planet. Inter. 13 (4), 260–267.

Didenko, A.N., Kurenkov, S.A., Lubnina, N.V., Simonov, V.A., 1998. Magnetic texture of intrusive rocks of the Voikaro-Syn'insk ophiolitic massif: estimation of stress fields, in: Urals. Fundamental Problems of Geodynamics and Stratigraphy [in Russian]. Nauka, Moscow, pp. 42–59.

Dobretsov, N.L., Borisenko, A.S., Izokh, A.E., Zhmodik, S.M., 2010. A thermochemical model of Eurasian Permo-Triassic mantle plumes as a basis for prediction and exploration for Cu–Ni–PGE and rare-metal ore deposits. Russian Geology and Geophysics (Geologiya i Geofizika) 51 (9), 903–924 (1159–1187).

Domyshev, V.G., 1974. Pyroclastic Formation, Trap Volcanism and Tectonics of the Southwestern Tunguska Syneclise [in Russian]. Nauka, Novosibirsk.

Dragoni, M., Lanza, R., Tallarico, A., 1997. Magnetic anisotropy produced by magma flow; theoretical model and experimental data from Ferrar dolerite sills (Antarctica). J. Geophys. Int. 128 (1), 230–240.

Dunlop, D.J., 2002. Theory and application of the Day plot (M_{rs}/M_s versus H_{cr}/H_c) 1. Theoretical curves and tests using titanomagnetite data. J. Geophys. Res. 107 (B3). DOI:10.1029/2001JB000487.

Elkins-Tanton, L.T., 2005. Continental magmatism caused by lithospheric delamination, in: Foulger, G.R., Natland, J.H., Presnall, D.S., Anderson, D.L. (Eds.), Plates, Plumes and Paradigms. Princeton, Geol. Soc. Am., Spec. Pap. 388, pp. 449–462.

Ernst, R.E., 2014. Large Igneous Provinces. Cambridge University Press.

Ernst, R.E., Baragar, W.R.A., 1992. Evidence from magnetic fabric for the flow pattern of magma in the Mackenzie giant radiating dyke swarm. Nature 356, 511–513.

Fedorenko, V., Czamanske, G., 1997. Results of new field and geochemical studies of the volcanic and intrusive rocks of the Maymecha-Kotuy area, Siberian flood-basalt province, Russia. Int. Geol. Rev. 39 (6), 479–531.

Fedorenko, V.A., Lightfoot, P.C., Naldrett A.J., Czamanske, G.K., Hawkesworth, C.J., Wooden, J.L., Ebel, D.S., 1996. Petrogenesis of the flood-basalt sequence at Noril'sk, North Central Siberia. Int. Geol. Rev. 38 (2), 99–135.

Feoktistov, G.D., 1976. Trap extending sills in the south of the Siberian Platform. Sovetskaya Geologiya 12, 122–127.

Feoktistov, G.D., 1978. Petrology and Conditions of Trap Sills Formation [in Russian]. Nauka, Novosibirsk.

Ferre, E.C., 2002. Theoretical models of intermediate and inverse AMS fabrics. Geophys. Res. Lett. 29 (7), 31-1–31-4. DOI: 10.1029/2001GL014367.

Fristad, K.E., Svensen, H.H., Polozov, A., Planke, S., 2017. Formation and evolution of the end-Permian Oktyabrsk volcanic crater in the Tunguska Basin, Eastern Siberia. Palaeogeogr. Palaeoclimatol. Palaeoecol. 468, 76–87.

Galerne, C.Y., Neumann, E.-R., Planke, S., 2008. Emplacement mechanisms of sill complexes: Information from the geochemical architecture of the Golden Valley Sill Complex, South Africa. J. Volcanol. Geotherm. Res. 177 (2), 425–440. DOI: 10.1016/j.jvolgeores.2008.06.004.

Hargraves, R.B., Johnson, D., Chan, C.Y., 1991. Distribution anisotropy: The cause of AMS in igneous rocks? Geophys. Res. Lett. 18 (12), 2193–2196.

Heunemann, C., Krasa, D., Soffel, H., Gurevitch, E., Bachtadse, V., 2004. Directions and intensities of the Earth's magnetic field during a reversal: results from the Permo-Triassic Siberian trap basalts, Russia. Earth Planet. Sci. Lett. 218 (1–2), 197–213.

Hoyer, L., Watkeys, M.K., 2017. Using magma flow indicators to infer flow dynamics in sills. J. Structural Geol. 96, 161–175. DOI: 10.1016/j.jsg.2017.02.005.

Hrouda, F., Buriánek, D., Krejčí, O., Chadima, M., 2015. Magnetic fabric and petrology of Miocene sub-volcanic sills and dikes emplaced into the SW Flysch Belt of the West Carpathians (S Moravia, Czech Republic) and their volcanological and tectonic implications. J. Volcanol. Geotherm. Res. 290, 23–38.

Ivanov, A.V., 2007. Evaluation of different models for the origin of the Siberian Traps, in: Foulger, G.R., Jurdy, D.M. (Eds.), Plates, Plumes and Planetary Processes. Geol. Soc. Am., Spec. Pap. 430, pp. 669–691.

Ivanov, A.V., Rasskazov, S.V., Feoktistov, G.D., He, H., Boven, A., 2005. $^{40}Ar/^{39}Ar$ dating of Usol'skii sill in the southeastern Siberian Traps Large Igneous Province: evidence for long-lived magmatism. Terra Nova 17 (3), 203–208.

Ivanov, A.V., He, H., Yang, L., Nikolaeva, I.V., Palesskii, S.V., 2009. $^{40}Ar/^{39}Ar$ dating of intrusive magmatism in the Angara-Taseevskaya syncline and its implication for duration of magmatism of the Siberian Traps. J. Asian Earth Sci. 35 (1), 1–12.

Ivanov, A.V., He, H., Yan, L., Ryabov, V.V., Shevko, A.Y., Palesskii, S.V., Nikolaeva, I.V., 2013. Siberian Traps large igneous province: evidence for two flood basalt pulses around the Permo–Triassic boundary and in the Middle Triassic, and contemporaneous granitic magmatism. Earth-Sci. Rev. 122, 58–76.

Jelínek, V., 1981. Characterization of the magnetic fabric of rocks. Tectonophysics 79 (3–4), T63–T67.

Jelínek, V., Kropáček, V., 1978. Statistical processing of anisotropy of magnetic susceptibility measures on groups of specimens. Studia Geophis. Geodet. 22 (1), 50–62.

Kamo, S.L., Czamanske, G.K., Amelin, Yu., Fedorenko, V.A., Davis, D.W., Trofimov, V.R., 2003. Rapid eruption of Siberian flood-volcanic rocks and evidence for coincidence with the Permian–Triassic boundary and mass extinction at 251 Ma. Earth Planet. Sci Lett. 214, 75–91.

Khan, M.A., 1962. The anisotropy of magnetic susceptibility of some igneous and metamorphic rocks. J. Geophys. Res. 67 (7), 2873–2885.

King, S.D., Anderson, D.L., 1998. Edge-driven convection. Earth Planet. Sci. Lett. 160 (3–4), 289–296. DOI: 10.1016/S0012-821X(98)00089-2.

Knight, M.D., Walker, G.P.L., 1988. Magma flow directions in dikes of the Koolau Complex, Oahu, determined from magnetic fabric studies. J. Geophys. Res. 93 (B5), 4301–4319.

Konstantinov, K.M., Bazhenov, M.L., Fetisova, A.M., Khutorskoy, M.D., 2014a. Paleomagnetism of trap intrusions, East Siberia: Implications to flood basalt emplacement and the Permo-Triassic crisis of biosphere. Earth Planet. Sci. Lett. 394, 242–253.

Konstantinov, K.M., Mishenin, S.G., Tomshin, M.D., Kornilova, V.P., Koval'chuk, O.E., 2014b. Petromagnetic inhomogeneities of the Permo-Triassic traps of the Daldyn-Aalakit diamond-bearing district (western Yakutia). Litosfera, No. 2, 77–98.

Krivolutskaya, N.A., 2013. Evolution of Trap Magmatism and Pt–Cu–Ni Mineralization in the Norilsk Region [in Russian]. Partnership Nauchnoe Izd. KMK, Moscow.

Kurenkov, S.A., Didenko, A.N., Simonov, V.A., 2002. Geodynamics of Paleospreading [in Russian]. GEOS, Moscow.

Latyshev, A.V., Veselovskiy, R.V., Ivanov, A.V., Fetisova, A.M., Pavlov, V.E., 2013. Short intense bursts in magmatic activity in the south of Siberian Platform (Angara-Taseeva depression): the paleomagnetic evidence. Izvestiya. Phys. Solid Earth 49 (6), 823–835.

Latyshev, A.V., Veselovskiy, R.V., Ivanov, A.V., 2018. Paleomagnetism of the Permian-Triassic intrusions from the Tunguska syncline and the Angara–Taseeva depression, Siberian Traps Large Igneous Province: Evidence of contrasting styles of magmatism. Tectonophysics 723, 41–55. DOI:10.1016/j.tecto.2017.11.035.

Magee, C., Muirhead, J.D., Karvelas, A., Holford, S.P., Jackson, C.A.L., Bastow, J.D., Schofield, N., Stevenson, C.T.E., McLean, C., McCarthy, W., Shtukert, O., 2016. Lateral magma flow in mafic sill complexes. Geosphere 12 (3), 809–841. DOI:10.1130/GES01256.1.

Malthe-Sørenssen, A., Planke, S., Svensen, H., Jamtveit, B., 2004. Formation of saucer-shaped sills, in: Breitkreuz, C., Petford, N. (Eds.), Physical Geology of High-Level Magmatic Systems. Geol. Soc. London, Spec. Publ. 234, pp. 215–227. DOI: 10.1144/GSL.SP.2004.234.01.13.

Naumov, V.A., Ankudimova, L.A., 1995. Palynological complexes and age of volcanogenic deposits in the Angara–Katanga region (Angara middle reaches). Geologiya i Geofizika (Russian Geology and Geophysics) 36 (1), 39–45 (37–43).

O'Driscoll, B., Ferre, E.C., Stevenson, S.T.E., Magee, C., 2015. The significance of magnetic fabric in layered mafic-ultramafic intrusions, in: Charlier, B., Namur, O., Latypov, R., Tegner, Ch. (Eds.), Layered Intrusions. Springer, pp. 295–329.

Park, J.K., Tanczyk, E.I., Desbarats, A., 1988. Magnetic fabric and its significance in the 1400 Ma Mealy diabase dykes of Labrador, Canada. J. Geophys. Res. 93 (B11), 13,689–13,704.

Paton, M.T., Ivanov, A.V., Fiorentini, M.L., McNaughton, N.J., Mudrovska, I., Reznitskii, L.Z., Demonterova, E.I., 2010. Late Permian and Early Triassic magmatic pulses in the Angara–Taseeva syncline,

Southern Siberian Traps and their possible influence on the environment. Russian Geology and Geophysics (Geologiya i Geofizika) 51 (9), 1012–1020 (1298–1309).

Polteau, S., Mazzini, A., Galland, O., Planke, S., Malthe-Sørenssen, A., 2008. Saucer-shaped intrusions: Occurrences, emplacement and implications. Earth Planet. Sci. Lett. 266 (1–2), 195–204. DOI: 10.1016/j.epsl.2007.11.015.

Polteau, S., Hendricks, B.W.H., Planke, S., Ganerod, M., Corfu, F., Faleide, J.I., Midtkandal, I., Svensen, H.S., Myklebust, R., 2016. The Early Cretaceous Barents Sea Sill Complex: distribution, $^{40}Ar/^{39}Ar$ geochronology, and implications for the carbon gas formation. Palaeogeogr. Palaeoclimatol. Palaeoecol. 441 (1), 83–95.

Potter, D.K., Stephenson, A., 1988. Single-domain particles in rocks and magnetic fabric analysis. Geophys. Res. Lett. 15 (10), 1097–1100.

Raposo, M.I.B., Ernesto, M., 1995. Anisotropy of magnetic susceptibility in the Ponta Grossa dyke swarm (Brazil) and its relationship with magma flow directions. Phys. Earth Planet. Inter. 87 (3–4), 183–196.

Reichow, M.K., Pringle, M.S., Al'Mukhamedov, A.I., Allen, M.B., Andreichev, V.L., Buslov, M.M., Davies, C., Fedoseev, G.S., Fitton, J.G., Inger, S., Medvedev, A.Ya., Mitchell, C., Puchkov, V.N., Safonova, I.Yu., Scott, R.A., Saunders, A.D., 2009. The timing and extent of the eruption of the Siberian Traps large igneous province: Implications for the end-Permian environmental crisis. Earth Planet. Sci. Lett. 277 (1–2), 9–20.

Rochette, P., Aubourg, C., Perrin, M., 1999. Is this magnetic fabric normal? A review and case studies in volcanic formations. Tectonophysics 307 (1–2), 219–234.

Rochette, P., Jenatton, L., Dupuy, C., Boudier, F., Reuber, I., 1991. Diabase dikes emplacement in the Oman ophiolite: a magnetic fabric study with reference to geochemistry, in: Peters, T., Nicolas, A., Coleman, R.G. (Eds.), Ophiolite Genesis and Evolution of the Oceanic Lithosphere, Proc. Ophiolite Conf., Muscat, Oman (7–18 January 1990). Springer, pp. 55–82.

Saunders, A., Reichow, M., 2009. The Siberian Traps and the end-Permian mass extinction: a critical review. Chin. Sci. Bull. 54 (1), 20–37.

Saunders, A.D., England, R.W., Reichow, M.K., White, R.V., 2005. A mantle plume origin for the Siberian traps: uplift and extension in the West Siberian Basin, Russia. Lithos 79 (3–4), 407–424. DOI: 10.1016/j.lithos.2004.09.010.

Schofield, N.J., Brown, D.J., Magee, C., Stevenson, C.T., 2012. Sill morphology and comparison of brittle and non-brittle emplacement mechanisms. J. Geol. Soc. 169, 127–141. DOI: 10.1144 /0016-76492011-078.

Shcherbakov, V.P., Latyshev, A.V., Veselovskiy, R.V., Tselmovich, V.A., 2017. Origin of false components of NRM during conventional stepwise thermal demagnetization. Russian Geology and Geophysics (Geologiya i Geofizika) 58 (9), 1118–1128 (1407–1421).

Sholpo, L.E., 1977. Magnetism of Subsurface Rocks for Solution of Geological Problems [in Russian]. Nedra, Leningrad.

Sholpo, L.E., Rusinov, B.Sh., Ilaev, M.G., Igoshin, L.A., Panfilov, V.A., Belykh, B.E., Burov, B.V., Glevasskaya, A.M., Dortman, N.B., Dubinchik, E.Ya., Zotova, I.F., Luzyanina, E.N., Mikhailova, N.P., Molostovskii, E.A., Pisakin, B.N., Popov, M.G., Rzhevskii, Yu.S., Rozental', I.V., Fainberg, F.S., Shevlyagin, E.V., Shchekin, V.N., 1986. Magnetism of Subsurface Rocks for Geological Survey [in Russian]. Nedra, Leningrad.

Sobolev, S.V., Sobolev, A.V., Kuzmin, D.V., Krivolutskaya, N.A., Petrunin, A.G., Arndt, N.T., Radko, V.A., Vasiliev, Y.R., 2011. Linking mantle plumes, large igneous provinces, and environmental catastrophes. Nature 477, 312–316. DOI: 10.1038/nature10385.

Svensen, H., Planke, S., Polozov, A.G., Schmidbauer, N., Corfu, F., Podladchikov, Y.Y., Jamtveit, B., 2009. Siberian gas venting and the end-Permian environmental crisis. Earth Planet. Sci. Lett. 277 (3–4), 490–500.

Svensen, H., Corfu, F., Polteau, S., Hammer, Ø., Planke, S., 2012. Rapid magma emplacement in the Karoo Large Igneous Province. Earth Planet. Sci. Lett. 325–326, 1–9.

Tarling, D.H., Hrouda, F., 1993. The Magnetic Anisotropy of Rocks. Chapman, Hall, London.

Tauxe, L., Gee, J.S., Staudigel, H., 1998. Flow directions in dikes from anisotropy of magnetic susceptibility data: the bootstrap way. J. Geophys. Res. 103 (B8), 17,775–17,790.

Varga, J.V., Gee, J.S., Staudigel, H., Tauxe, L., 1998. Dike surface lineations as magma flow indicators within the sheeted dike complex of the Troodos Ophiolite, Cyprus. J. Geophys. Res. 103 (B3), 5241–5256.

Editorial responsibility: D.V. Metelkin